Phase behaviour in binary mixtures of ultrasoft repulsive particles

To cite this article: S. D. Overduin and C. N. Likos 2009 *EPL* **85** 26003

A LETTERS JOURNAL EXPLORING
THE FRONTIERS OF PHYSICS

January 2009

EPL, **85** (2009) 26003
doi: `10.1209/0295-5075/85/26003`

`www.epljournal.org`

Phase behaviour in binary mixtures of ultrasoft repulsive particles

S. D. OVERDUIN[a] and C. N. LIKOS

Institute for Theoretical Physics II: Soft Matter, Heinrich-Heine-Universität Düsseldorf - Universitätsstraße 1, D-40225 Düsseldorf, Germany, EU

received 4 November 2008; accepted in final form 22 December 2008

PACS `64.70.D-` – Solid-liquid transitions
PACS `61.20.Gy` – Theory and models of liquid structure
PACS `82.30.Nr` – Association, addition, insertion, cluster formation

Abstract – We investigate the phase behaviour of binary mixtures consisting of two ultrasoft species labeled 1 and 2, using the liquid-state theory and the classical density functional theory. The interaction potentials of the two species belong to different classes of ultrasoft potentials that display a dramatically different phase behaviour in the pure case: in the pure species-1 system, there is a maximum freezing temperature and re-entrant melting occurs; in the pure species-2 system, freezing to a cluster-crystal phase, defined by multiple occupancy of each lattice site, occurs at all temperatures. We examine the phase behaviour in the mixture for different potential parameters. In some cases we find that the clustering behaviour of species 2 can induce clustering of species 1 in 2-rich systems. We identify and characterise stable crystal structures and investigate the effect of a nearby demixing transition on the liquid-solid phase coexistence.

Introduction. – The competition between macrophase and microphase separation in classical systems is a common phenomenon that depends delicately on the details of the interparticle interactions. The question arises both in the context of one-component systems and in that of binary mixtures. In the former case, examples are offered by colloidal particles that entail a short-range attraction and a long-range repulsion [1], the former being caused by, *e.g.*, depletion effects due to added polymer chains and the latter by the presence of residual charges, screened by counterions and salt [2–12]. In the above works, it has been demonstrated that, depending on the range and strength of the attractive and repulsive parts, the liquid-gas binodal can be completely suppressed, giving rise to the formation of clusters in an otherwise homogeneous fluid. Even in the complete absence of long-range repulsions, macrophase separation can be rendered metastable with respect to sublimation, provided the attraction range is short enough [13–18]. Block coploymer solutions are another example in which the competition between antagonistic, attractive and repulsive forces, can tip the scales from macrophase separation to micelle formation, depending on the relative lengths of the blocks and the polymer architecture [19–22].

For binary mixtures, the situation is richer since there are now three interaction potentials at play. For hard-sphere mixtures, it has been shown that demixing is suppressed by crystallization [23,24], whereas colloid-polymer mixtures, described at the level of the Asakura-Oosawa-Vrij model, show macroscopic demixing, provided the polymer size exceeds, roughly, 40% of that of the colloids [25]. A novel class of interactions, which has drawn considerable attention to it in the realm of soft matter physics, are *ultrasoft* potentials, which are free of divergences, and which model effective potentials between polymeric colloids of various architectures [26]. In this context, Gaussian mixtures, modeling polymer blends, have been studied and it has been demonstrated that the cross-interaction between the two species plays a crucial role in determining whether macrophase separation [27–31] or microphase ordering [31,32] will occur. However, novel phenomena can show up when, for example, the ultrasoft potential decays more sharply than the Gaussian potential [33] (*i.e.* $\exp[-(r/\sigma)^m]$, where $m > 2$), in which case at least one of the two components involved has a Kirkwood instability in its fluid structure and thus undergoes a transition to cluster crystals at sufficiently high densities [33–38]. The purpose of this work is to investigate the phase behaviour scenarios that appear in such mixtures. We demonstrate that several instability lines are simultaneously present in the mixture,

---

[a] E-mail: `overduin@thphy.uni-duesseldorf.de`

both for infinite- and finite-wavelength perturbations of the uniform state, giving thus rise to competition between demixing and ordering in super-clustered crystals. The phase behaviour is *extremely* sensitive to the form of the cross-interaction between the two species in a binary mixture. We accompany the phase diagrams with structural information on the two species, calculated within an accurate density functional theory approach.

The model. – We consider systems of particles interacting through the generalised exponential model (GEM-m),

$$u_{ij}(r) = \epsilon_{ij} \exp\left[-\left(r/\sigma_{ij}\right)^{m_{ij}}\right]. \tag{1}$$

Evidently, the model involves nine parameters, the three energy scales ϵ_{ij}, the three length scales σ_{ij} and the three exponents m_{ij}, $i,j=1,2$. Choosing one of the ϵ_{ij} as the unit of energy and one of the σ_{ij} as the unit of length, still leaves us with seven model parameters. In addition, the concentration of the second species, $x \equiv \rho_2/\rho$, the total density $\rho = \rho_1 + \rho_2$ as well as the temperature T are the thermodynamic parameters of the many-body system, rendering thereby the whole parameter space highly dimensional. To simplify things, we focus at the dependence of the phase diagram on the relative range of the cross-interaction σ_{12}, varying the density ρ and the concentration x and keeping all other parameters fixed. In particular, we choose $\epsilon_{ij} = \epsilon$, $(i,j=1,2)$, and $\sigma_{11} = \sigma_{22} = \sigma$.

In order to make a choice for the exponents m_{ij} of the interactions, we recall some established facts on the phase behaviour of the GEM-m model in general [35]. The Fourier transform of the GEM-m potential is positive everywhere when $m \leqslant 2$, and the GEM-($m \leqslant 2$) potential belongs to the Q^+ class; pure Q^+ systems are characterised by the presence of a maximum freezing temperature and the occurrence of re-entrant melting [39–44]. Simulation results show that the effective potential between two polymer chains in isolation [45,46], or between two athermal dendrimers [47] in isolation, can be modeled by a Q^+-potential, specifically the GEM-2 potential. The Fourier transform of the GEM-m potential oscillates around zero when $m > 2$, and thus the GEM-($m > 2$) potential belongs to the $Q^\pm$ class of potentials; pure $Q^\pm$ systems freeze at all temperatures and form a cluster-crystal phase [34–36,48]. Recent computer simulation results show that the isolated effective potential between two dendrimers with amphiphilic end groups [49], can be modeled by a $Q^\pm$ potential of the GEM-m form.

Although cluster-crystal formation does not occur in a pure GEM-2 system, theoretical work suggests that a highly delocalised cluster-crystal may form in a mixture of two GEM-2 species [32], due to the appearance in the mixture of a λ-instability line (see below), on which the structure factors of the uniform fluid phase diverge at a nonzero value of the wave number. The λ-line of the Gaussian mixture is a combined effect of all three interparticle interaction potentials, since it is absent for any of the two pure components. In what follows, we study a system consisting of GEM-2 ($m_{11}=2$) and GEM-4 ($m_{22}=4$) particles, as a model $Q^+/Q^\pm$ mixture. Contrary to the Gaussian mixture, here the pure GEM-4 component has an instability line of its own. We aim at exploring the significance of this fact on the phase behaviour of the mixture as well as the possibilities of emergence of *additional* instability lines due to the presence of both components. We choose the exponent in the cross-interaction potential to belong to the $Q^\pm$ class, $m_{12}=3$. This choice is motivated by the fact that in a mixture of athermal (GEM-2) and amphiphilic (GEM-4) dendrimers, the cross-interaction will have, in general, an exponent lying in-between the two and, as the GEM-2 lies at the threshold of the Q^+-class, the cross-interaction will classify as $Q^\pm$. In this sense, the precise choice $m_{12}=3$ is at this point arbitrary but the ensuing phenomena should be generic.

Method and results. – In all investigations, we work at *fixed* temperature $k_\mathrm{B}T/\epsilon = 1$, where k_B is Boltzmann's constant. The liquid direct correlation functions of the two components, $c_{ij}(r)$, $i,j=1,2$, can be approximated within the mean-field approximation (MFA)

$$c_{ij}(r) = -\beta u_{ij}(r), \tag{2}$$

and used as a closure to the the Ornstein-Zernike (OZ) equation to obtain the total correlation function $h_{ij}(r)$,

$$h_{ij}(r) = c_{ij}(r) + \sum_l \rho_l \int \mathrm{d}^3 r' h_{il}(r') c_{lj}(|\mathbf{r}-\mathbf{r}'|), \tag{3}$$

where $\beta = (k_B T)^{-1}$, and ρ_l is the bulk number density of species l. The MFA has been shown to be very accurate for systems interacting through ultrasoft potentials at high density [32,35,40,50].

The partial structure factors $S_{ij}(k)$ are related to the Fourier transform of the total correlation function $\tilde{h}_{ij}(k)$,

$$S_{ij}(k) = \delta_{ij} + \sqrt{\rho_i \rho_j}\,\tilde{h}_{ij}(k); \tag{4}$$

the divergence of $S_{ij}(k)$ signals fluid instability. In Fourier space, the OZ can be written as

$$\tilde{h}_{ij}(k) = \frac{N_{ij}(k)}{D(k)}, \tag{5}$$

where, within the MFA, the denominator can be written in terms of the Fourier transforms of the potentials $\tilde{u}_{ij}(k)$,

$$\begin{aligned} D(k) \;=\; & 1 + \beta\left[\rho_1 \tilde{u}_{11}(k) + \rho_2 \tilde{u}_{22}(k)\right] \\ & -\rho_1\rho_2\beta^2\left[\tilde{u}_{12}^2(k) - \tilde{u}_{11}(k)\tilde{u}_{22}(k)\right]. \end{aligned} \tag{6}$$

The partial structure factors diverge when $D(k)=0$; divergence occurs for some density and concentration when either of the following two conditions is true: $\tilde{u}_{ii}(k) < 0$, or $\tilde{u}_{11}(k)\tilde{u}_{22}(k) < \tilde{u}_{12}^2(k)$. The first condition is satisfied for

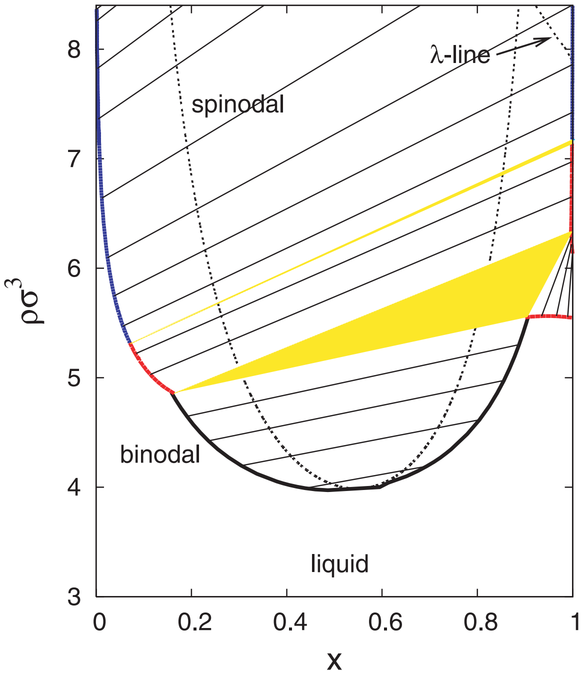

Fig. 1: (Colour on-line) Phase diagram for a system with $\sigma_{12} = 1.07$. The black lines represents the λ- and spinodal lines, and the thick lines denote the boundaries of the coexistence regions: liquid-liquid (black), liquid-BCC (red) and liquid-FCC (dark blue). The thin lines join coexisting points. The three-phase coexistence areas are denoted by the yellow triangles. The BCC-FCC coexistence area is very small and can be taken to be the point where the thick red and blue curves meet.

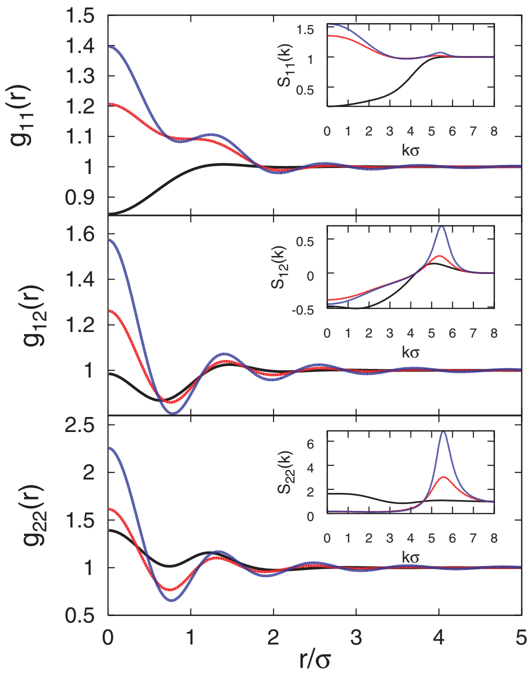

Fig. 2: (Colour on-line) The air correlation functions $g_{ij}(r)$ and the partial structure factors $S_{ij}(k)$ (insets), for a system with $\sigma_{12} = 1.07\,\sigma$ at the following densities and concentrations: $\rho = 5.5$ and $x = 0.1$ (black); $\rho = 5.5$ and 0.95 (red); $\rho = 7.0$ and 0.95 (dark blue). The partial structure factors demonstrate how near each fluid is to instability.

some $k > 0$ when, as is our case, the interaction potential of one of the species belongs to the $Q^{\pm}$ class and is related to the cluster-crystal formation in the pure system; a λ-line denotes the locus of points where $D(k \neq 0) = 0$. The second condition can be satisfied for any value of k; when satisfied at $k = 0$, demixing occurs, and the spinodal denotes the locus of points where $D(k = 0) = 0$.

We consider first a mixture with $\sigma_{12} = 1.07\,\sigma$. In fig. 1, we see that such a mixture features *two* instability lines: a λ-line, *i.e.*, $D(k^* \neq 0) = 0$, which has its origin at the Kirkwood instability of the pure GEM-4-model, and a demixing spinodal, *i.e.*, $D(k = 0) = 0$. On the high-density side of the two lines is the region of instability of the homogeneous fluid with respect to infinitesimal deviations of the two partial densities $\rho_i(\mathbf{r})$ from uniformity at wavelengths given by the values of k on the instability lines.

Of interest is the structure of the fluid as the system approaches the λ-line. In fig. 2, we show the pair correlation functions for this system and the structure factors (insets) to indicate how close the system is to a fluid instability. As the system approaches the λ-line, the peak in $g_{22}(r)$ at $r = 0$ increases, as expected. Interestingly, peaks in both $g_{11}(r)$ and $g_{12}(r)$ at $r = 0$ also appear, suggesting that the clustering behaviour of the GEM-4 species draws in the non-clustering GEM-2 species. The reason for this lies in the $Q^{\pm}$ nature of the cross-interaction potential; the GEM-2 species is "forced" into the GEM-4 clusters to minimise the number of GEM-4 particles that it overlaps with, and as a result, it also clusters with other GEM-2 particles. Further, the propensities of the two components to demix (maxima of $S_{ij}(k)$ at $k = 0$) or to microphase-order (maxima of $S_{ij}(k)$ at $k^* \neq 0$) can be discerned, where it can be seen that the relative height of the two is not the same for both species.

To determine the phase diagram, we follow the compressibility route to obtain the liquid excess Helmholtz free energy $(f^{ex}(\rho, x))$ per particle $(N = N_1 + N_2)$ as a function of density $\rho = (N_1 + N_2)/V$ and concentration $x = N_2/(N_1 + N_2)$, as outlined in refs. [29,50]. Briefly,

$$f^{ex}(\rho, x) = (1-x)^2 \beta \tilde{u}^0_{11} + 2x(1-x)\beta \tilde{u}^0_{12} + x^2 \beta \tilde{u}^0_{22}, \quad (7)$$

where $\tilde{u}^0_{ij}$ is the value of the Fourier transform of the potential at $k = 0$. The ideal contribution to the free energy $\beta f^{id}(\rho, x)$ contains an ideal gas term and the entropy-of-mixing term, $x \ln x + (1-x)\ln(1-x)$.

The properties of candidate solid phases are calculated using classical density functional theory (DFT) with the MFA-excess Helmholtz free energy [32,34]:

$$F_{ex}[\rho_i, \rho_j] = \frac{1}{2} \sum_{i,j=1}^{2} \int\!\!\int \mathrm{d}^3 r \mathrm{d}^3 r' \rho_i(\mathbf{r}) \rho_j(\mathbf{r}') u_{ij}(|\mathbf{r} - \mathbf{r}'|). \quad (8)$$

We make the Gaussian approximation for the one-particle density,

$$\rho_i(\mathbf{r}) \equiv n_i \left(\frac{\alpha_i}{\pi}\right)^{3/2} \sum_{\{\mathbf{R}\}} \exp\left[-\alpha_i(\mathbf{r}-\mathbf{R})^2\right], \qquad (9)$$

where n_i is the number of particles of species i at each lattice site, α_i is the delocalisation parameter and the sum is over all lattice sites $\{\mathbf{R}\}$. The ideal contribution to the free energy is given by:

$$F_{id}[\rho] = k_{\mathrm{B}}T \sum_{l=1}^{2} \int \mathrm{d}^3 r \rho_l(\mathbf{r}) \left[\ln(\rho_l(\mathbf{r})\Lambda_l^3) - 1\right], \qquad (10)$$

where Λ_l is the thermal de Broglie wavelength of species l.

The excess part of the variational free energy per particle $\tilde{f}(\alpha_1, \alpha_2, n_1, n_2)$ is given by

$$\begin{aligned}\tilde{f}_{ex} = \frac{1}{2}\sum_{i,j=1}^{2}\Bigg[& x_i n_j \left(\frac{\chi_{ij}}{\pi}\right)^{1/2} \sum_{m=1}^{\infty} \xi_m \\ & \times \int_0^{\infty} \mathrm{d}r \frac{r}{R_m}\left[e^{-\chi_{ij}(r-R_m)^2} - e^{-\chi_{ij}(r+R_m)^2}\right] u_{ij}(r) \\ & + x_i n_j \left(\frac{16\chi_{ij}^3}{\pi}\right)^{1/2} \int_0^{\infty} r^2 e^{-\chi_{ij} r^2} u_{ij}(r)\mathrm{d}r \Bigg], \qquad (11)\end{aligned}$$

where $\chi_{ij} = \alpha_i\alpha_j/(\alpha_i+\alpha_j)$ and R_m denotes the lattice vectors lengths. The sum in the right-hand side of eq. (11) above runs thus over all *nonvanishing* Bravais lattice vectors $\mathbf{R}$, ordered according to their length, so that ξ_m is the number of vectors participating in the shell with length R_m. The contribution to the free energy from the particles occupying *the same* lattice site is expressed by the last term in eq. (11). The free energy of the (meta)stable solid phase is determined by minimizing eq. (11) with respect to α_1, α_2 and the lattice spacing d. Note that n_i can be obtained from d and ρ_i through $n_i = \rho_i d^3/\zeta$, where ζ is the number of lattice sites per cubic cell. The second term in the above equation accounts for the interparticle interactions at one lattice site; here we multiplied by n_j rather than $n_j - 1$ in order to maintain consistency with the compressibility route used to calculate the free energies of the liquid phase. Equation (11) reduces to the liquid Helmholtz free-energy calculated via the compressibility route, when $\alpha_1 = \alpha_2 = 0$. The compositions of coexisting phases is determined by using the double-tangent construction on the Gibbs free energy per particle $g = f + P/\rho$ as described by Archer *et al.* [27,29,32].

As candidate solid structures we considered body-centered cubic (BCC) and face-centered cubic (FCC) lattices with all sites occupied by both species (mixed lattice), and NaCl- and CsCl-type structures, with different species located at alternating sites. We find that the BCC and FCC mixed lattices are the most stable structures for the systems considered in this work. This result is consistent with the peak in all $g_{ij}(r)$ at $r = 0$ discussed above; the GEM-2 particles are drawn into the GEM-4 clusters. However, the demixing tendency of the system only allows the mixed clusters to be stable over a very small concentration range, *i.e.*, $x > 0.99$. Although both species are centered on every lattice site, the GEM-2 species is much more delocalised than the GEM-4; the value of α_1 is roughly half the value of α_2. Thus, although the GEM-2 model shows no propensity to clustering whatsoever, and it possesses just one fluid state at this temperature [40], the presence of the GEM-4 component has a twofold influence on the Gaussian particles: on the one hand, it enforces a macrophase separation; on the other, the GEM-4 clusters that spontaneously form at $x = 1$ act as "nucleation centers" for the minority Gaussian particles, which now occupy the *same* crystal sites as the GEM-4 ones in a multiply clustered "supercrystal" with mixed occupancy of its lattice sites. Due to the weaker localization of the Gaussian particles on the crystal sites, it can be expected that their long-time diffusivity will be considerably larger than that of the GEM-4 ones [37], thus giving rise to a crystal with markedly different mobilities between its two components.

For a system with $\sigma_{12} = 1.07\sigma$, liquid-liquid demixing occurs for total densities in the range $4 \lesssim \rho\sigma^3 \lesssim 5$. At higher densities, the demixing transition is preempted, first by the liquid-solid BCC transition, and then by the liquid-solid FCC transition. There are two triple regions in this system: the BCC solid phase coexists with both a fluid phase rich in species 2 and a fluid phase rich in species 1, and at a higher density a fluid rich in species 1 coexists with both a BCC and an FCC solid phase. The repulsion between the two species dictates that the mixed clusters cannot be stable for very large concentrations of species 1. Therefore, the solid, highly concentrated in species 2 ($x > 0.99$), coexists with the fluid phase in order to satisfy both the requirement that the number of overlapping species 1 and 2 particles be minimised and that the concentration of the cluster accommodate the unfavorable interaction between the two species.

To investigate the influence of the cross-interaction range on the structural and phase behaviour of the mixture, we compare the results for a system with $\sigma_{12} = 1.07\sigma$ discussed above to those obtained for a system with a slightly decreased range: $\sigma_{12} = 1.05\,\sigma$. The latter system also has a λ-line associated with the GEM-4 cluster-crystal formation, and a spinodal. However, macrophase separation is here preempted by crystallization, a feature brought about by a *minimal* reduction of the cross-interaction range. Furthermore, the spinodal lies within a second λ-line, as shown in fig. 3. The latter is reminiscent of that observed for a GEM-2 mixture [32] where the λ-line occurs in a system that does not demix at any density. However, whereas for the GEM-2 mixture a negative non-additivity of the interactions, *i.e.*, $\epsilon_{12} < \epsilon_{11} = \epsilon_{22}$ *and* $\sigma_{12} < (\sigma_{11} + \sigma_{22})/2$ is necessary to bring about such an instability, here this is not the case. This second λ-line moves inside of the

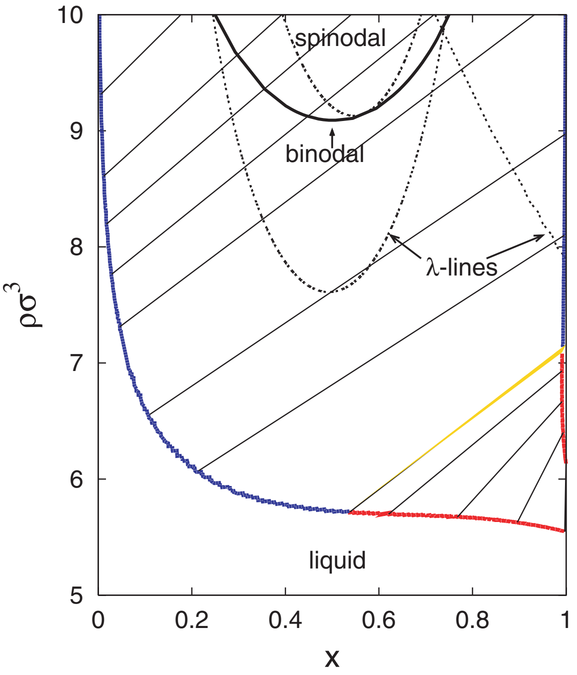

Fig. 3: (Colour on-line) Phase diagram for a system with $\sigma_{12} = 1.05\,\sigma$. The broken lines represents the λ- and spinodal lines, and the thick lines denote the boundaries of the coexistence regions: liquid-BCC (red), liquid-FCC (dark blue) and the metastable liquid-liquid coexistence (black), which is preempted by the liquid-solid transition. The thin lines join coexisting points. The three-phase coexistence is represented by the yellow triangle.

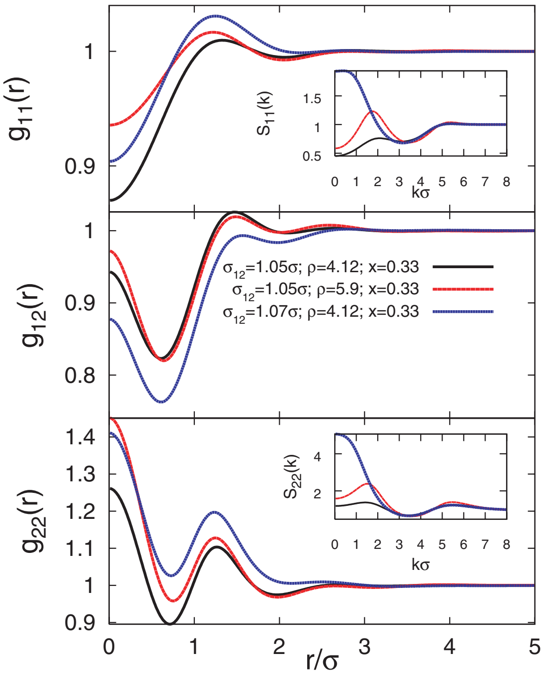

Fig. 4: (Colour on-line) A comparison between the partial correlation functions of the demixing system ($\sigma_{12} = 1.07\,\sigma$) with those of the non-demixing one ($\sigma_{12} = 1.05\,\sigma$) at characteristic points of the corresponding phase diagrams.

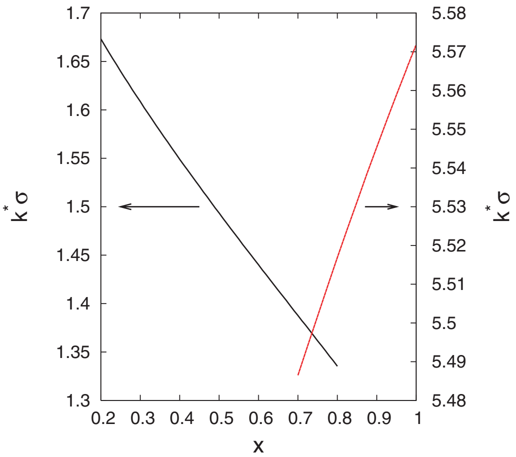

Fig. 5: (Colour on-line) The values k^* of the wave numbers at which instabilities occur along the two λ-lines of the mixture without a macrophase separation. Right vertical axis: the λ-line dictated by the GEM-4 components; left vertical axis: the new λ-line.

spinodal as the range of repulsion between the two species increases and is present at higher densities, for the system with $\sigma_{12} = 1.07\,\sigma$ discussed above. For the system with $\sigma_{12} = 1.05\,\sigma$, there is a region where the preference of each species to interact with itself is not strong enough to result in demixing but does result in an unstable homogeneous liquid phase. While one might expect this to lead to a second solid structure, in this case, the liquid- solid coexistence associated with the original λ-line, is very broad and preempts the formation of a second solid structure.

In fig. 4 we show a comparison of the correlation functions between the mixture with $\sigma_{12} = 1.07\,\sigma$ and that with $\sigma_{12} = 1.05\,\sigma$. Although little difference can be seen in the radial distribution functions $g_{ij}(r)$, the Fourier-space analysis on the basis of the partial structure factors $S_{ij}(k)$ brings about the salient differences: whereas the former system shows enhanced forward scattering ($k = 0$), the latter shows peaks at a finite value $k = k^*$, which is clearly distinct from that associated with the Kirkwood instability of the GEM-4-model. Indeed, as can be seen in fig. 5, the second λ-line corresponds to instabilities at wave numbers that are smaller than the first by as much as a factor 4; correspondingly, it describes the propensity of the system to form novel cluster crystals with a lattice constant as much as 4 times bigger than that of the pure GEM-4 crystals. Though these are not stable for the model at hand ($\sigma_{12} = 1.05\,\sigma$), it can be anticipated that they will gain stability if the cross-interaction range is further reduced. The kind of ordering between the two species that would occur in such crystals is a problem for the future.

Summary and conclusions. – We have examined by means of an accurate density functional theory the structural and phase behaviour in mixtures between clustering and non-clustering, ultrasoft particles. The interplay between demixing and crystallization is reminiscent of the scenarios for one-component systems, however the physics is here much richer. Further, there seems to be an extreme sensitivity of the ensuing phase behaviour to the interaction parameters. We have found the existence of mixed cluster crystals, in which the minority, non-clustering component, collapses on the crystal sites occupied by the clustering one. Future work should focus on the possibilities to bring the second λ-line down to lower densities, so as to make novel, possibly intercalated, crystals stable. Investigations on the wetting behaviour of the demixing system across the coexistence line, of mixed crystals in confined geometries, on triple-point melting and on the issue of partial diffusivities, are additional problems for future work.

* * *

SDO is grateful for the financial support of the Natural Sciences and Engineering Research Council of Canada.

REFERENCES

[1] Sear R. P. and Gelbart W. M., *J. Chem. Phys.*, **110** (1999) 4582.

[2] Stradner A., Sedgwick H., Cardinaux F., Poon W. C. K., Egelhaaf S. U. and Schurtenberger P., *Nature*, **432** (2004) 492.

[3] Sciortino F., Mossa S., Zaccarelli E. and Tartaglia P., *Phys. Rev. Lett.*, **93** (2004) 055701.

[4] Mossa S., Sciortino F., Tartaglia P. and Zaccarelli E., *Langmuir*, **20** (2004) 10756.

[5] Campbell A. I., Anderson V. J., van Duijneveldt J. S. and Bartlett P., *Phys. Rev. Lett.*, **94** (2005) 208301.

[6] Imperio A. and Reatto L., *J. Phys.: Condens. Matter*, **16** (2004) S3769.

[7] Imperio A. and Reatto L., *J. Chem. Phys.*, **124** (2006) 164712.

[8] Stiakakis E., Petekidis G., Vlassopoulos D., Likos C. N., Iatrou H., Hadjichristidis N. and Roovers J., *Europhys. Lett.*, **72** (2005) 664.

[9] Charbonneau P. and Reichmann D. R., *Phys. Rev. E*, **75** (2007) 011507.

[10] Archer A. J. and Wilding N. B., *Phys. Rev. E*, **76** (2007) 031501.

[11] Archer A. J., *Phys. Rev. E*, **78** (2008) 031402.

[12] Archer A. J., Ionescu C., Pini D. and Reatto L., *J. Phys.: Condens. Matter*, **20** (2008) 415106.

[13] Mederos L. and Navascués G., *J. Chem. Phys.*, **101** (1994) 9841.

[14] Daanoun A., Tejero C. F. and Baus M., *Phys. Rev. E*, **50** (1994) 2913.

[15] Coussaert T. and Baus M., *Phys. Rev. E*, **52** (1995) 862.

[16] Tejero C. F., Daanoun A., Lekkerkerker H. N. W. and Baus M., *Phys. Rev. Lett.*, **73** (1994) 752.

[17] Tejero C. F., Daanoun A., Lekkerkerker H. N. W. and Baus M., *Phys. Rev. E*, **51** (1995) 558.

[18] Hasegawa M., *J. Chem. Phys.*, **108** (1998) 208.

[19] Panagiotopoulos A. Z., Floriano M. A. and Kumar S., *Langmuir*, **18** (2002) 2940.

[20] Pierleoni C., Addison C., Hansen J.-P. and Krakoviack V., *Phys. Rev. Lett.*, **96** (2006) 128302.

[21] Lo Verso F., Panagiotopoulos A. Z. and Likos C. N., *Phys. Rev. E*, **79** (2009) 010401.

[22] Abbas S. and Lodge T. P., *Phys. Rev. Lett.*, **97** (2006) 097803.

[23] Dijkstra M., van Roij R. and Evans R., *Phys. Rev. E*, **59** (1999) 5744.

[24] Velasco E., Navascués G. and Mederos L., *Phys. Rev. E*, **60** (1999) 3158.

[25] Dijkstra M., Brader J. M. and Evans R., *J. Phys.: Condens. Matter*, **11** (1999) 10079.

[26] Likos C. N., *Phys. Rep.*, **348** (2001) 267.

[27] Archer A. J. and Evans R., *Phys. Rev. E*, **64** (2001) 041501.

[28] Archer A. J. and Evans R., *J. Phys.: Condens. Matter*, **14** (2002) 1131.

[29] Archer A. J., Likos C. N. and Evans R., *J. Phys.: Condens. Matter*, **14** (2002) 12031.

[30] Finken R., Hansen J.-P. and Louis A. A., *J. Stat. Phys.*, **110** (2003) 1015.

[31] Finken R., Hansen J.-P. and Louis A. A., *J. Phys. A: Math. Gen.*, **37** (2004) 577.

[32] Archer A. J., Likos C. N. and Evans R., *J. Phys.: Condens. Matter.*, **16** (2004) L297.

[33] Likos C. N., Lang A., Watzlawek M. and Löwen H., *Phys. Rev. E*, **63** (2001) 031206.

[34] Mladek B. M., Gottwald D., Kahl G., Neumann M. and Likos C. N., *Phys. Rev. Lett.*, **96** (2006) 045701.

[35] Likos C. N., Mladek B., Gottwald D. and Kahl G., *J. Chem. Phys.*, **126** (2007) 224502.

[36] Mladek B. M., Charbonneau P. and Frenkel D., *Phys. Rev. Lett.*, **99** (2007) 235702.

[37] Moreno A. J. and Likos C. N., *Phys. Rev. Lett.*, **99** (2007) 107801.

[38] van Teeffelen S., Moreno A. J. and Likos C. N., to be published in *Soft Matter*, **5** (2009) DOI: 10.1039/b813916d.

[39] Stillinger F. H. and Stillinger K. D., *Physica A*, **244** (1997) 358.

[40] Lang A., Likos C. N., Watzlawek M. and Löwen H., *J. Phys.: Condens. Matter*, **12** (2000) 5087.

[41] Prestipino S., Saija F. and Giaquinta P. V., *Phys. Rev. E*, **71** (2005) 050102.

[42] Saija F. and Giaquinta P. V., *ChemPhysChem*, **6** (2005) 1768.

[43] Prestipino S., Saija F. and Giaquinta P. V., *J. Chem. Phys.*, **123** (2005) 144110.

[44] Archer A. J., *Phys. Rev. E*, **72** (2006) 051501.

[45] Krüger B., Schäfer L. and Baumgärtner A., *Appl. Sci. Res.*, **22** (1970) 403.

[46] Dautenhahn J. and Hall C. K., *Macromolecules*, **27** (1994) 5399.

[47] Götze I. O., Harreis H. M. and Likos C. N., *J. Chem. Phys.*, **120** (2004) 77761.

[48] Mladek B. M., Gottwald D., Kahl G., Neumann M. and Likos C. N., *J. Phys. Chem. B*, **111** (2007) 12799.

[49] Mladek B. M., Kahl G. and Likos C. N., *Phys. Rev. Lett.*, **100** (2008) 028301.

[50] Louis A. A., Bolhuis P. and Hansen J., *Phys. Rev. E*, **62** (2000) 7961.